Carbohydrate Polymers 92 (2013) 1880–1886

Contents lists available at SciVerse ScienceDirect

Carbohydrate Polymers

journal homepage: www.elsevier.com/locate/carbpol

Cytotoxicity and antibacterial ability of scaffolds immobilized by polysaccharide/layered silicate composites

Shangjing Xin[a,b,1], Xueyong Li[c,1], Zhaocheng Ma[d], Zhanjun Lei[c], Jiemin Zhao[b], Siyi Pan[b], Xue Zhou[a,**], Hongbing Deng[b,*]

[a] State Key Laboratory of Environment Health (Incubation); Key Laboratory of Environment and Health, Ministry of Education; Key Laboratory of Environment and Health (Wuhan), Ministry of Environmental Protection; Department of Occupational and Environmental Health, School of Public Health, Tongji Medical College, Huazhong University of Science and Technology, Wuhan 430030, China
[b] College of Food Science and Technology, Huazhong Agricultural University, No. 1 Shizishan Road, Wuhan 430070, China
[c] Department of Plastic Surgery, Tangdu Hospital, Fourth Military Medical University, Xi'an, 710038, China
[d] College of Horticulture and Forestry Sciences, Huazhong Agricultural University, No. 1 Shizishan Road, Wuhan 430070, China

ARTICLE INFO

Article history:
Received 17 July 2012
Received in revised form 30 August 2012
Accepted 14 November 2012
Available online 23 November 2012

Keywords:
Chitosan
Pectin
Layer-by-layer
Antibacterial
Cytotoxicity

ABSTRACT

Chitosan and pectin/organic rectorite (OREC) were initially deposited on the surface of cellulose acetate electrospun nanofibers by a layer-by-layer (LBL) technique to fabricate scaffolds for bacterial inhibition, and the cytotoxicity of the LBL structured scaffolds was also investigated. A couple of opposite charged material, pectin and OREC, were firstly used to fabricate the intercalated composites. The intercalated structure was determined by selected area electron diffraction. Field-emission scanning electron microscope, X-ray diffraction and X-ray photoelectron spectroscopy were applied for the characterization of LBL structured nanofibrous scaffolds. Antibacterial assay results showed that the diameters of the inhibition zone increased from 7.6 to 15.8 mm for *Escherichia coli*, as well as from 7.4 to 14.2 mm for *Staphylococcus aureus*. Finally, human epidermal (EP) cells grew well on the LBL films coating. These novel scaffolds could be an ideal candidate for wound dressings and food packaging.

1. Introduction

Recently, multilayered and multifunctional nanofibrous scaffolds fabricated via electrospinning and layer-by-layer (LBL) deposition technique are popular for wound dressings and food packaging (Huang et al., 2012; Khang, Carpenter, Chun, Pareta, & Webster, 2010; Schiffman & Schauer, 2008; Venugopal & Ramakrishna, 2005). Electrospun nanofibrous scaffolds have a 3D structure with pores in micro and sub-micro size and have been extensively applied in wound dressings due to their ultra-thin fiber diameter, small pore size and high specific surface-area-to-volume ratio (Ding, Wang, Wang, Yu, & Sun, 2010; Rujitanaroj, Pimpha, & Supaphol, 2008; Shalumon, Anulekha, Nair, Chennazhi, & Jayakumar, 2011; Wang, Liu, Xu, & Sun, 2011). Generally, a key design element for fabricating wound dressings or food packaging scaffolds is whether they can exhibit bacteria inhibition and biocompatibility (Zahedi, Rezaeian, Ranaei Siadat, Jafari, & Supaphol, 2010). Unfortunately, most natural polysaccharides with good electrospinnability do not possess these properties. An example is cellulose acetate (CA), which is easy to electrospin but with unsatisfactory biocompatibility and poor antibacterial properties (Deng et al., 2010). In this case, the LBL technique can be an essential and effective method to modify the surface of CA nanofibrous scaffolds by depositing biopolymers.

Chitosan (CS), a partially deacetylated derivative of chitin, is abundant in crustacean outer skeletons and positively charged (Yang, Chou, & Li, 2002). It exhibits excellent biocompatibility, biodegradability and permeability, and has been applied for drug delivery, bacterial inhibition and tissue engineering (Deng et al., 2010, 2012; Xu et al., 2013). Several reports have shown that chitosan is an ideal candidate for wound dressings because its antibacterial properties and stimulation of cell proliferation are specially useful for wound treatment (Ong, Wu, Moochhala, Tan, & Lu, 2008; Zhang, Yang, & Nie, 2008). The adhesive nature of chitosan and its permeability to oxygen is also a very important property associated with wound dressings (Jayakumar, Prabaharan, Kumar, Nair, & Tamura, 2011).

Pectin (PT) is a natural, non-toxic and anionic polysaccharide found in the cell walls of most plants (Chong, Simsek, & Reuhs, 2009; Pagán, Ibarz, Llorca, Pagán, & Barbosa-Cánovas, 2001). Pectin extracts are widely used in the food processing industry due to its well known thickening and gelling properties (Coimbra et al.,

* Corresponding author. Tel.: +86 27 87282111; fax: +86 27 87282111.
** Corresponding author. Tel.: +86 27 83693280; fax: +86 27 83693280.
E-mail addresses: xue.zhou@hust.edu.cn (X. Zhou), alphabeita3000@yahoo.com.cn (H. Deng).
[1] Co-first author with the same contribution to this work.

0144-8617/$ – see front matter © 2012 Elsevier Ltd. All rights reserved.
http://dx.doi.org/10.1016/j.carbpol.2012.11.040

2011). Furthermore, pectin is effective in bacterial inhibition and with good biocompatibility (Girod Fullana, Ternet, Freche, Lacout, & Rodriguez, 2010; Tripathi, Mehrotra, & Dutta, 2010). Therefore, pectin has drawn much attention in drug delivery and tissue engineering (Coimbra et al., 2011; Lin & Yeh, 2010).

Organic rectorite (OREC), one kind of layered silicate, has been applied for antibacterial activity, drug controlled-release ability and gene delivery (Deng et al., 2012; Wang, Pei, Du, & Li, 2008; Xu et al., 2013). Based on our previous report, the addition of OREC into nanofibers can enhance bacterial inhibition because the interlayer of OREC can be intercalated by chains of biopolymers and more positively charged surface can be exposed to kill the bacterial cell (Deng et al., 2011). In addition, OREC has already been shown to have low cytotoxicity to normal cells when immobilized in nanofibers (Xin et al., 2012). Based on the previous results of related literatures above, it is reasonable to hypothesize that the interlayer space of OREC can be intercalated with the chains of pectin.

Both chitosan and pectin, however, are not able to be electrospun directly. In this case the LBL technique is necessary for depositing these materials on template nanofibrous scaffolds templates. In this study, we initially determined the Zeta-potential of chitosan (34.1 mV), pectin (−26.0 mV), OREC (10.8 mV), pectin–OREC composites (−26.4 mV) and CA templates (−28.3 mV). Positively charged chitosan and negatively charged pectin or pectin–OREC composites were deposited on CA nanofibrous scaffolds alternatively. Field-emission scanning electron microscope (FE-SEM), selected area electron diffraction (SAED), X-ray diffraction (XRD) and X-ray photoelectron spectroscopy (XPS) were utilized to characterize LBL films assembled nanofibrous scaffolds. The bacterial inhibition activity was measured by the inhibition zone method. Finally, an evaluation of the in vitro biocompatibility activity on human epidermal (EP) cells of LBL structured nanofibrous scaffolds was performed by MTT assay and cell culture experiments.

2. Materials and methods

2.1. Materials

Chitosan (CS, $M_w = 2.0 \times 10^5$ kD) from shrimp shell with 92% deacetylation was from Zhejiang Yuhuan Ocean Biochemical Co., China. Pectin (PT, galacturonic acid ≥74.0%) extracted from citrus peel was supplied by Sigma–Aldrich Co., USA. Cellulose acetate (CA, $M_n = 3 \times 10^4$ kD) was purchased from Sigma–Aldrich Co., USA. Calcium rectorite (Ca^{2+}-REC) was provided by Hubei Mingliu Co., China. Organic rectorite was prepared based on a previous report (Wang, Du, Yang, Shi, & Hu, 2006). All other chemicals were of analytical grade and used as received. All aqueous solutions were prepared by using purified water with a resistance of 18.2 MΩ cm.

2.2. Fabrication of LBL nanofibrous scaffolds

CA nanofibers were fabricated via electrospinning technique for 24 h and the electric field was 15 kV/15 cm. Pectin solution was added dropwise and slowly into OREC suspensions at 60 °C under gentle agitation for 12 h to obtain mixed solutions. Pectin–OREC composites had a mass ratio of pectin and OREC of 20:1. The deposition materials for LBL modification were positively charged chitosan (1 mg/mL) solution and negatively charged pectin or pectin–OREC intercalated composites (1 mg/mL) solution. The former was dissolved by acetic acid and the latter was prepared by purified water. The pH value of chitosan was adjusted to 5.0 and that of pectin (or pectin–OREC composites) was adjusted to 4.0 by diluted HCl and NaOH solutions. The ionic strength of the layer solutions was regulated by the addition of NaCl at a concentration of 0.1 M.

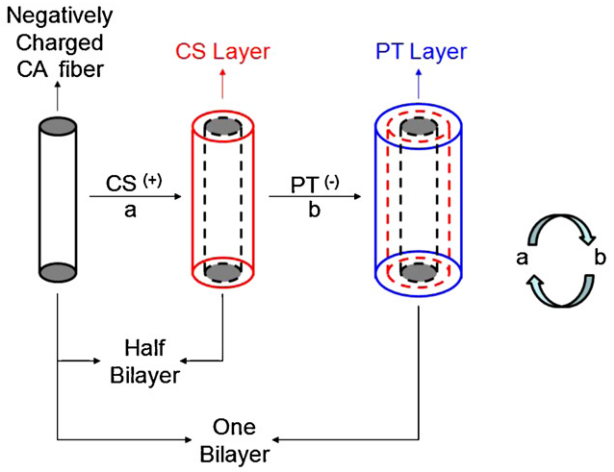

Fig. 1. Schematic diagram illustrating the fabrication process of LBL structured nanofibrous scaffolds.

The concept for the fabrication of LBL structured fibrous scaffolds is shown in Fig. 1. Briefly, CA nanofibers (8 cm × 8 cm) were firstly soaked into chitosan solution for 20 min and then immersed into pectin or pectin–OREC solutions for 20 min. Before immersing into another solution the system was rinsed for 2 min in pure water three times. After these depositions in the two solutions, the bilayer was coated. Here, $(CS/PT)_n$ or $(CS/PT–OREC)_n$ was used as a formula to label the LBL structured films, where n was the number of the coating bilayers. The outermost layer was chitosan when n equaled to 5.5 and 10.5, as well as 5 and 10 denoted that pectin or pectin–OREC was on the outmost layer. The LBL structured nanofibrous scaffolds were dried at 60 °C for 24 h under vacuum prior to further characterizations.

2.3. Characterization

Zeta potentials of the bulk materials for LBL process were measured by a Zetasizer 3690 (Malvern, UK). The morphology of the LBL structured nanofibrous scaffolds was observed by field emission scanning electron microscope (JSM-6700F, JEOL, Japan). Pectin–OREC intercalated composites were investigated by selected area electron diffraction (JEM-2100, JEOL, Japan). The composition of composite nanofibrous scaffolds was examined by XPS using an axis ultra DLD apparatus (Kratos, UK). XRD was performed using X'Pert Pro (PANalytical, Netherlands).

2.4. Bacterial inhibition ability test

Inhibition zone method was used to investigate the inhibitory effect of the LBL structured nanofibrous scaffolds against Gram-negative bacteria *Escherichia coli* and Gram-positive bacteria *Staphylococcus aureus*. 50 μL bacteria levitation liquid with the concentration of $5.0–10.0 \times 10^5$ cfu/mL was added into a meat-peptone broth. LBL films coated scaffolds disks (diameter = 6 mm) were sterilized at 120 °C for 30 min, and then were tiled to cling to the bacteria levitation liquid. After incubation at 37 °C for 12 h, the inhibition zones were measured with a tolerance of 1 mm. Three parallel experiments were carried out for each sample.

2.5. MTT assay

The cytotoxicity of the LBL films deposited scaffolds was measured using MTT method based on a previous report (Zhao et al., 2009). The scaffolds cultivated with human epidermal cells (1×10^3) by Dulbecco modified eagle medium (DMEM) were

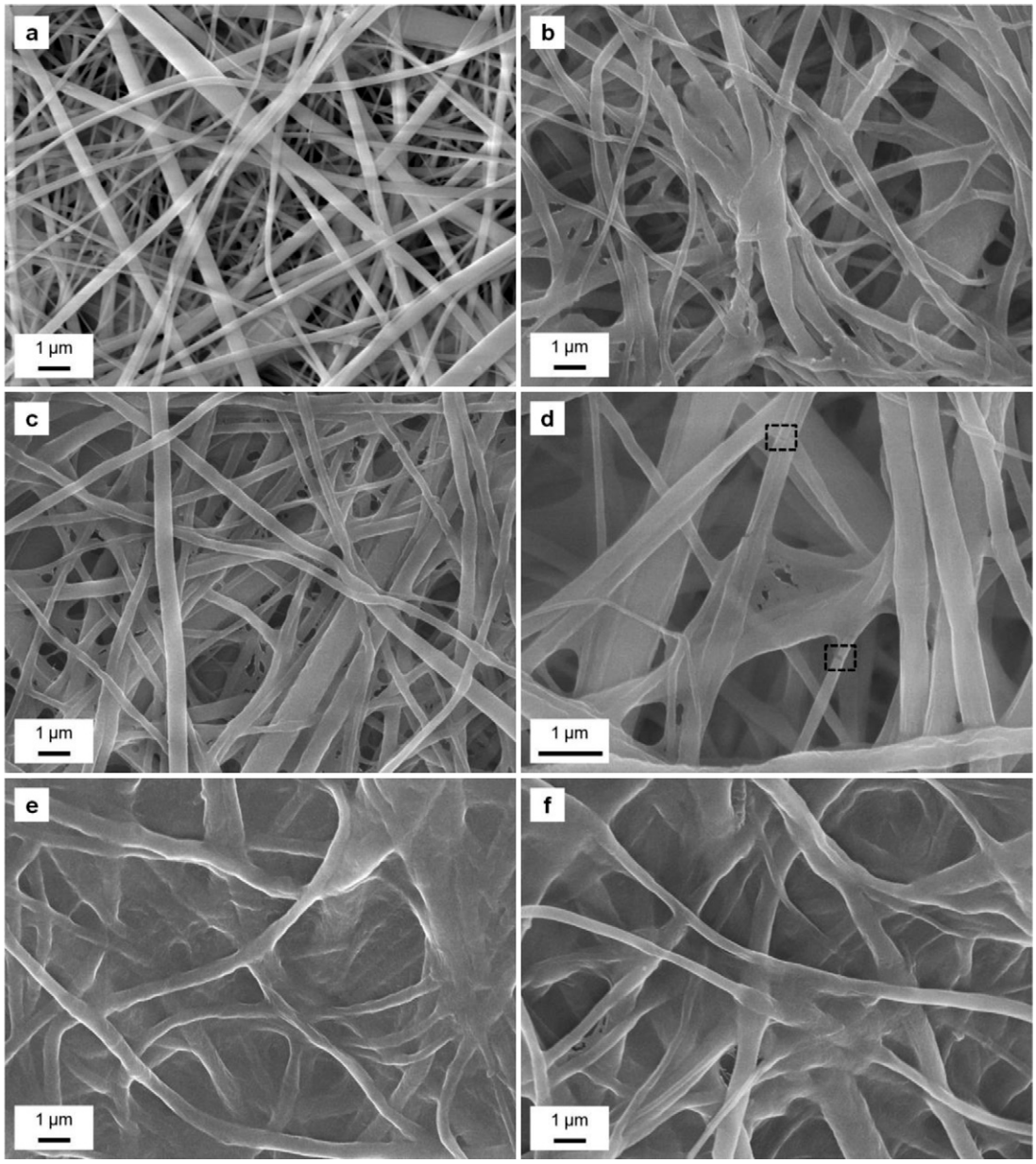

Fig. 2. FE-SEM images of (a) CA nanofibers and LBL structured nanofibrous scaffolds coated with: (b) $(CS/PT)_5$, (c) $(CS/PT)_{5.5}$, (d) $(CS/PT–OREC)_{5.5}$, (e) $(CS/PT)_{10}$ and (f) $(CS/PT)_{10.5}$.

washed slightly by phosphate buffered saline (PBS). Then MTT (25 μL) was added into each plate at 37 °C for 4 h. After that, DMSO (150 μL) was added to dissolve the MTT formazan purple crystals. Finally, the absorbance of the solution was measured at 490 nm by using an enzyme linked immunosorbent assay (ELISA) Reader (MODEL550, Bio-Rad, USA). The results were presented as the mean ± standard deviation (SD). Significant difference, which was measured by the Bonferroni's post hoc test, was performed using one-way analysis of variance (ANOVA). Values of $^{*}p < 0.05$ and $^{***}p < 0.01$ were considered significant.

2.6. Cellular fluorescence assay

The LBL structured scaffolds were cut into small disks to fit the size of 96-well plates and then sterilized by high pressure at 121 °C. EP cells (1×10^3) in DMEM were seeded onto the scaffolds in the 96-well plates, respectively. DMEM was supplemented with 10% fetal bovine serum (FBS) and 1% penicillin/streptomycin. Cells grew at 37 °C in an incubator with a humidified atmosphere containing 5% CO_2 for 24 h or 72 h. Live/dead viability/cytotoxicity kit (L3224, Molecular Probes Inc., USA) was used to detect the viability of cells and observed by confocal laser scanning microscope (LSM, 510 META, Zeiss, Germany). The polyanionic dye calcein was excited with a laser at 495 nm, and detected with a 515 longpass filter, and EthD-1 was excited with a 495 nm laser and detected with a 635 longpass filter.

3. Results and discussion

3.1. The morphology of LBL fibrous scaffolds

The morphology of the CA fibers and LBL films assembled fibrous scaffolds was observed by FE-SEM (Fig. 2). The average diameter of CA fibers was about 400 nm and their surface was smooth (Fig. 2a). After LBL films deposition, the average diameter of fibers increased and distributed between 600 and 800 nm. Besides, the

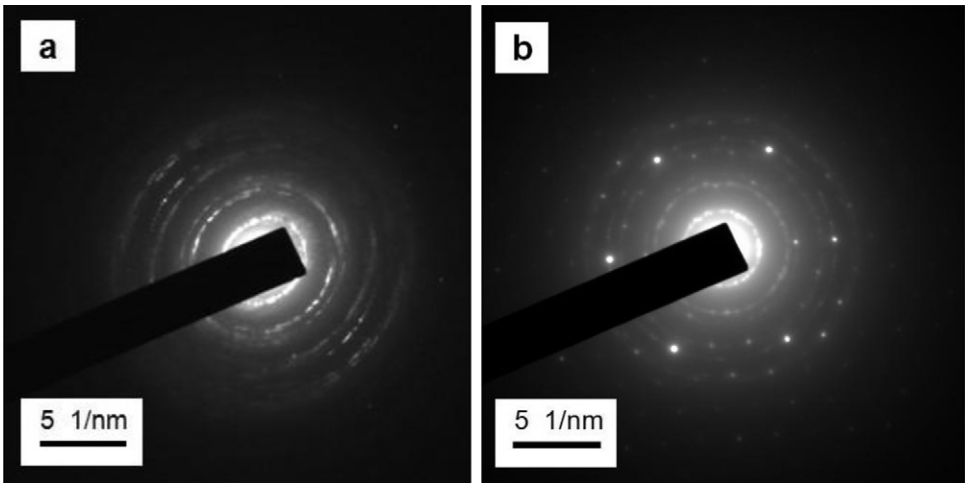

Fig. 3. SAED patterns of OREC powder and PT–OREC composites (20:1).

fibers became adjacent and their surfaces were coarse after deposition which indicated that polymers were assembled on the CA fibers and shrunk onto the surface after drying. $(CS/PT)_5$ and $(CS/PT)_{5.5}$ films coated scaffolds almost exhibited similar diameters and surface morphology, while the deposition space among the adhesive fibers in the scaffolds differed from each other, which might result in the imbalance of the deposition speed among the fibers. In Fig. 2b, many fibers were knotted which was ascribed to the stickiness of pectin and also proved that negatively charged pectin could attach on the fibers followed by positively charged chitosan. In addition, when pectin–OREC composites were chosen as the negatively charged deposition layer, OREC clay particles could successfully interact with CA fibers outlined by the rectangles in Fig. 2d. All these dark spots were of approximate 100 nm size and showed that OREC was well dispersed in the scaffolds.

In Fig. 2e and f, when the number of the coating bilayers was 10 and 10.5, the CA fibers were strongly embedded into pectin films formed after drying and the fibrous structure tended to disappear. The reason was that a large amount of pectin would adhere on the surface of the fibers and take the spaces among the scaffolds, which could affect the 3D structured CA nanofibrous scaffolds. Therefore, for keeping good nanofibrous structure during LBL process, the number of bilayers was adjusted at 5 or 5.5 rather than 10 or 10.5. The FE-SEM images verified that the LBL modification by chitosan and pectin was successful.

3.2. Diffraction studies

SAED patterns were used to determine the intercalation structure between the pectin chains and the interlayer of OREC (Fig. 3). The diameters of diffraction rings in Fig. 3b were slightly smaller than that in Fig. 3a. According to the Bragg's equation, the result verified that the interlayer distance of OREC enlarged by the intercalation of pectin chains successfully. The pectin chains might coat on the surface of OREC, or insert into the interlayer of it. In addition, the intensity of the diffraction rings in Fig. 3b slightly decreased, which indicated that the crystallization of both OREC and pectin was destroyed because the molecular movement of pectin chains was restricted between the interlayer of OREC. The result further indicated that the intercalated composites were successfully fabricated. Moreover, there were some diffraction points with regular arrangement and high intensity in Fig. 3b, elucidating that part of OREC became monocrystal structure.

X-ray diffractograms of bulk materials and LBL films coatings were displayed in Fig. 4. Chitosan exhibited two characteristic peaks around $2\theta = 10^\circ$ and 19°, and pectin had two peaks at $2\theta = 12.8^\circ$ and 20.6°. They both showed broad peaks especially for the smaller diffraction angles, thereby indicating that long range disorder was found in polymer samples (Tripathi et al., 2010). The diffractograms of LBL structured nanofibrous scaffolds were similar to that of CA nanofibrous scaffolds, but the peak at $2\theta = 8^\circ$ was intensified and shifted to larger angle which verified that CA nanofibers had strong interactions with chitosan and pectin chains. Furthermore, the height, width and position of peaks between $(CS/PT)_{5.5}$ and $(CS/PT–OREC)_{5.5}$ films coated CA scaffolds were different. Compared with $(CS/PT)_{5.5}$ films coating, $(CS/PT–OREC)_{5.5}$ films coating showed a relatively narrow peak. As we know, the width of X-ray diffraction peak was related to the size of crystallite, so the broadened peak was caused by OREC which had a narrow peak at $2\theta = 8^\circ$. Therefore, the result proved that chitosan and pectin had greatly changed the crystal structure of CA templates and OREC was successfully added into the LBL films modified scaffolds.

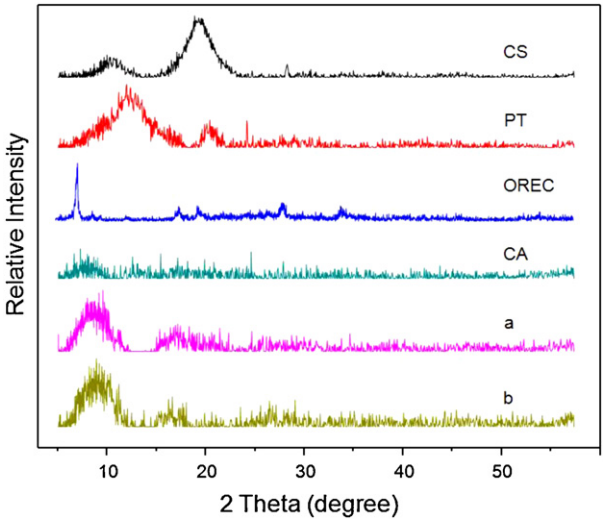

Fig. 4. XRD patterns of CS, PT, OREC powder, CA nanofibers and LBL structured nanofibrous scaffolds coated with: (a) $(CS/PT)_{5.5}$ and (b) $(CS/PT–OREC)_{5.5}$.

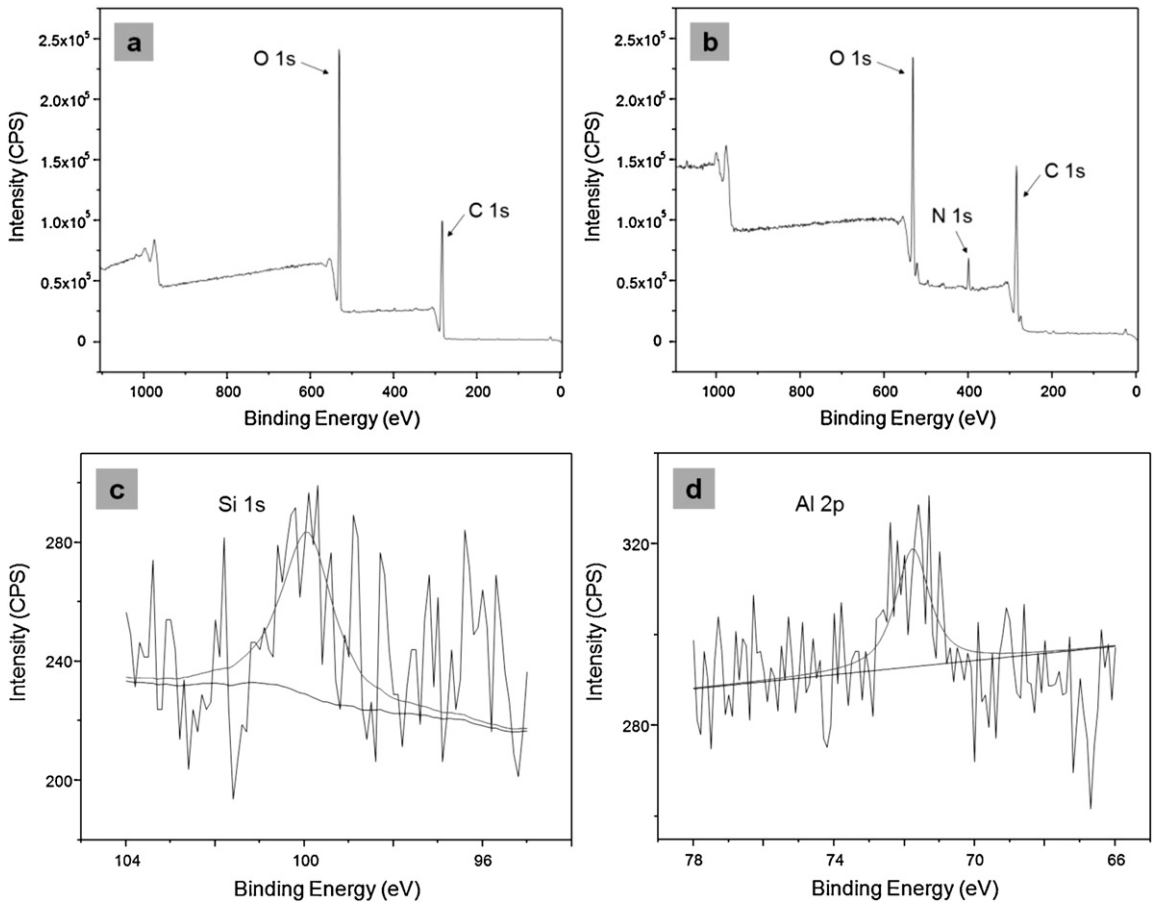

Fig. 5. XPS narrow scans with the curve fit of: (a) CA nanofibers and LBL structured nanofibrous scaffolds modified with: (b) $(CS/PT)_{0.5}$ and $(CS/PT–OREC)_{5.5}$: (c) Si 1s and (d) Al 2p.

3.3. Composition analysis of LBL structured nanofibrous scaffolds

The elemental composition of LBL structured nanofibrous scaffolds was investigated by XPS in Fig. 5. The main elements of CA were carbon and oxygen (Fig. 5a). To our knowledge, the characteristic elements of chitosan and OREC were nitrogen and silicon or aluminum, respectively, while pectin mainly consisted of carbon and oxygen. In Fig. 5b, the amount of nitrogen was 5.87% which demonstrated that chitosan was assembled on the surface of CA nanofibers. The peak of nitrogen was around 398.8 eV corresponding to C—N—C which verified that chitosan had interacted with CA (Park, Jung, Cho, & Choi, 2006). Besides, the dominant peak of silicon was at 100.0 eV (Fig. 5c) which was close to the value measured on pure silicon surfaces (Rosso, Giesbers, Arafat, Schroën, & Zuilhof, 2009). The dominant peak of aluminum was at 72.4 eV (Fig. 5d) which showed that Al was mainly in the metallic state (Zhou, Wang, & Xue, 2011). These two peaks elucidated that OREC existed in the LBL films coated scaffolds. XPS spectroscopy indicated that LBL structured scaffolds were successfully fabricated.

3.4. Antibacterial assay

The inhibition ability of the composite nanofibrous scaffolds against *E. coli* and *S. aureus* was measured via inhibition zone surrounding circular disks and the results were shown in Fig. 6. CA nanofibrous scaffold showed little bacterial inhibition activity. However, the diameter of inhibition zone increased remarkably after LBL deposition of chitosan and pectin on the surface of CA scaffolds. Several previous reports had already verified that both chitosan and pectin could inhibit bacteria effectively (Chen, Kung, Chen, & Lin, 2010; Tripathi et al., 2010). When pectin was on the outmost layer, the inhibition zone of *S. aureus* was larger compared to chitosan which indicated that pectin had a better property in Gram positive bacterial inhibition and the better solubility of pectin than chitosan might effectively make the scaffolds tightly stick on the broth. While chitosan was on the outmost layer, the scaffolds exhibited more effective inhibition activity against Gram negative bacterial.

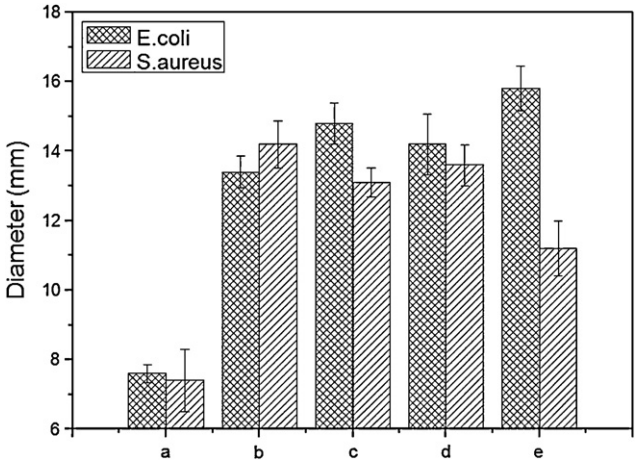

Fig. 6. Average diameters of bacterial growth inhibition zone against *E. coli* and *S. aureus* of: (a) CA nanofibers and LBL structured scaffolds coated with: (b) $(CS/PT)_5$, (c) $(CS/PT)_{5.5}$, (d) $(CS/PT–OREC)_5$ and (e) $(CS/PT–OREC)_{5.5}$.

The inhibition zone enlarged a lot after the deposition of pectin–OREC on the nanofibers. The main reason was that OREC was positively charged and could absorb the negatively charged bacteria cells so that the antibacterial activity would enhance. OREC and pectin are oppositely charged. After intercalation, these two could interact better because of the electrostatic force. OREC could absorb, and further inhibit the proliferation of bacteria on account of its significant surface area and adsorption capacities, and improve the antibacterial activity of nanofibrous scaffolds. From the SEM image, OREC particles were well dispersed onto the nanofibers. As the height of OREC particles was more than that of pectin coating, OREC would be still on the outmost layer after chitosan immobilization. Moreover, the cytotoxicity of the scaffolds would slightly increase even when chitosan was on the outmost layer. Therefore, LBL structured nanofibrous scaffolds, especially with the addition of OREC, results in excellent bacterial inhibition.

3.5. MTT assay

MTT assay results were shown to evaluate the cytotoxicity of LBL structured nanofibrous scaffolds to EP cells (Fig. 7). Obviously, all samples had little cytotoxicity because chitosan and pectin are both natural polysaccharides and are nontoxic. When chitosan was on the outmost layer, the viability of EP cells was highest which verified that chitosan had excellent biocompatibility. However, the OREC contained scaffolds exhibited a little cytotoxicity. Our previous study reported that the cytotoxicity of OREC could be ignored regarding to the improved properties of composites (Xin et al., 2012). Besides, the cytotoxicity of $(CS/PT–OREC)_{5.5}$ was lower than that of CA nanofibrous scaffolds. Therefore, natural polysaccharides depositing on CA nanofibers was an effective method to make the scaffolds biocompatible and OREC would not notably affect the biocompatibility of the scaffolds.

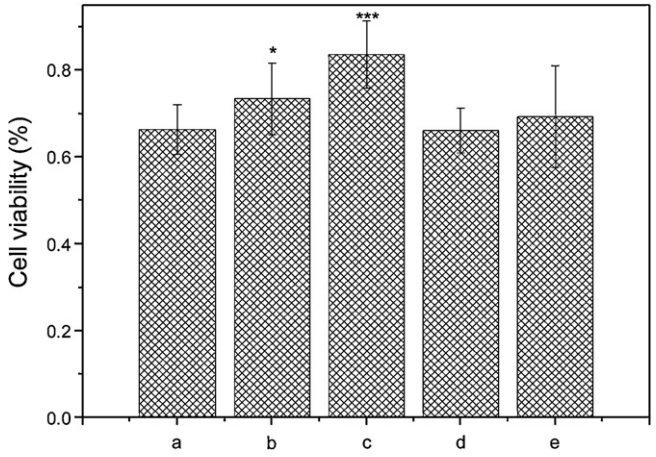

Fig. 7. MTT assay for the cell viability of EP cells on scaffolds of: (a) CA nanofirous scaffolds and LBL structured scaffolds deposited with: (b) $(CS/PT)_5$, (c) $(CS/PT)_{5.5}$, (d) $(CS/PT–OREC)_5$ and (e) $(CS/PT–OREC)_{5.5}$. Significant difference: $^{*}p < 0.05$, $^{***}p < 0.01$.

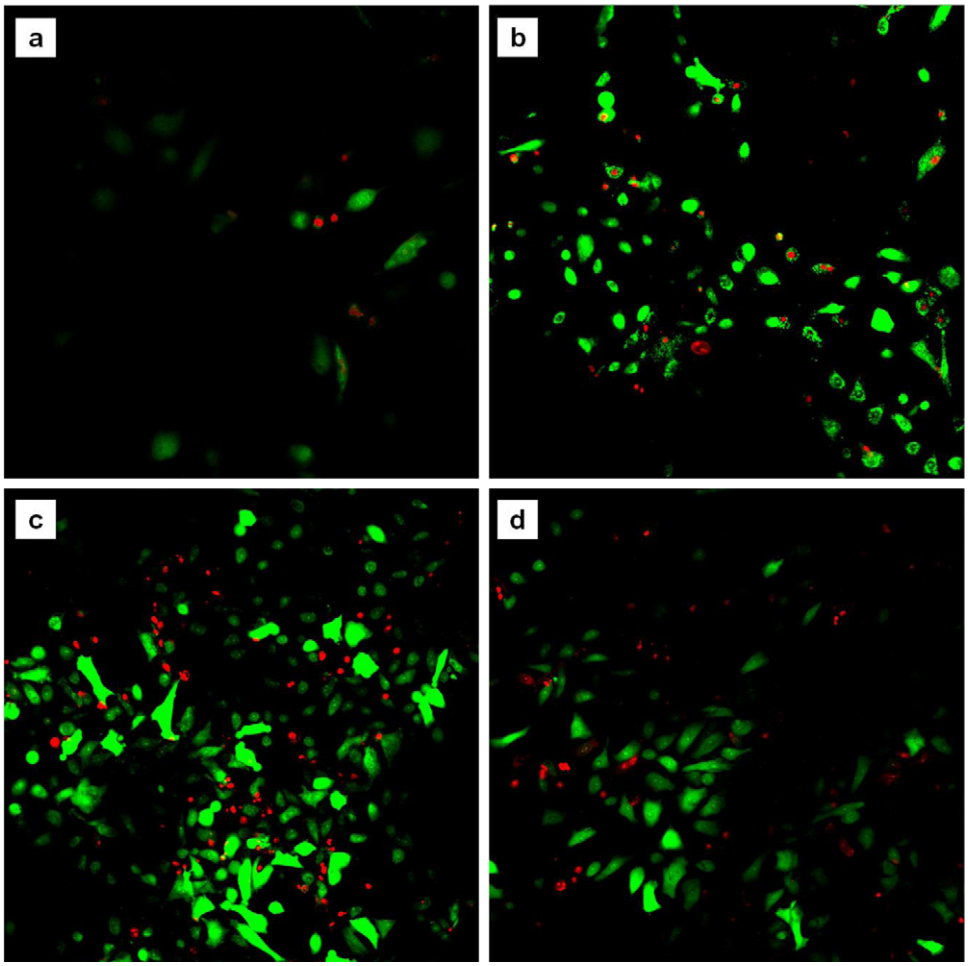

Fig. 8. Confocal microscope observation of cells cultured on: (a) CA nanofibrous mats and LBL structured scaffolds modified with: (b) $(CS/PT)_5$, (c) $(CS/PT)_{5.5}$ and (d) $(CS/PT–OREC)_{5.5}$.

3.6. Fluorescence staining assay

To further determine the cytotoxicity of the pristine and LBL films coating, the cellular apoptosis on the scaffolds was investigated by fluorescence staining with live/dead viability/cytotoxicity kit (Fig. 8). The green spots represented live cells while the red ones stood for dead cells because only if the cells became dead and the permeability of the cell membrane increased, the nucleus would be exposed and stained to red. CA nanofibrous scaffolds (Fig. 8a) had poor biocompatibility onto which only about 10 cells grew and most of them were dead. After LBL modification, when the outmost layer was pectin (Fig. 8b), the cells on the scaffolds exhibited round morphology and much more cells could be observed than those on CA template. Besides, most of them were alive which indicated that cells could survive onto pectin-coated nanofibrous scaffolds. When the outmost layer was chitosan (Fig. 8c), there were denser cells with flat morphology and obvious pseudopodes than those on the LBL structured scaffolds with the outmost layer of pectin. In addition, the ratio of live and dead cells increased which proved that chitosan had better biocompatibility and the cells began to split on the scaffolds in 24 h. After adding OREC (Fig. 8d), the cells grew also well on LBL structured nanofibrous scaffolds and most live cells exhibited flat morphology. However, the number of cells decreased, which confirmed that OREC had cytotoxicity in some degree but did not remarkably influence the growth of cells. This was identical with the results of MTT assay. The above results verified that LBL structured nanofibrous scaffolds were with excellent biocompatibility. Although adding OREC would affect the biocompatibility of the scaffolds, considering about the bacterial inhibition enhancement, this low cytotoxicity could be acceptable if the amount of OREC was limited.

4. Conclusion

In this work, chitosan and pectin–OREC were deposited on the CA nanofibrous scaffolds via LBL technique successfully. The bacterial inhibition ability of LBL structured nanofibrous scaffolds obviously enhanced and the biocompatibility was improved after the LBL assembly process. Besides, adding OREC would enhance antibacterial activity of the scaffolds while not strongly influencing the biocompatibility when its amount was limited. The novel scaffolds can be potentially utilized for wound dressings and food packaging.

Acknowledgements

We were very grateful to the staff from Department of Plastic Surgery, Tangdu Hospital, Fourth Military Medical University for the cell experiments assistance. This project was funded by National Natural Science Foundation of China (nos. 31101365 and 31000900) and Fundamental Research Funds for the Central Universities of China Huazhong Agricultural University, no. 52902-0900202208 and Huazhong University of Science and Technology, no. 2011QN206. Partially was supported by China Postdoctoral Science Foundation (20100471003).

References

Chen, L. C., Kung, S. K., Chen, H. H., & Lin, S. B. (2010). Evaluation of zeta potential difference as an indicator for antibacterial strength of low molecular weight chitosan. *Carbohydrate Polymers*, *82*, 913–919.

Chong, H. H., Simsek, S., & Reuhs, B. L. (2009). Analysis of cell-wall pectin from hot and cold break tomato preparations. *Food Research International*, *42*, 770–772.

Coimbra, P., Ferreira, P., De Sousa, H., Batista, P., Rodrigues, M., Correia, I., et al. (2011). Preparation and chemical and biological characterization of a pectin/chitosan polyelectrolyte complex scaffold for possible bone tissue engineering applications. *International Journal of Biological Macromolecules*, *48*, 112–118.

Deng, H., Li, X., Ding, B., Du, Y., Li, G., Yang, J., et al. (2011). Fabrication of polymer/layered silicate intercalated nanofibrous mats and their bacterial inhibition activity. *Carbohydrate Polymers*, *83*, 973–978.

Deng, H., Lin, P., Xin, S., Huang, R., Li, W., Du, Y., et al. (2012). Quaternized chitosan-layered silicate intercalated composites based nanofibrous mats and their antibacterial activity. *Carbohydrate Polymers*, *89*, 307–313.

Deng, H., Zhou, X., Wang, X., Zhang, C., Ding, B., Zhang, Q., et al. (2010). Layer-by-layer structured polysaccharides film-coated cellulose nanofibrous mats for cell culture. *Carbohydrate Polymers*, *80*, 474–479.

Ding, B., Wang, M., Wang, X., Yu, J., & Sun, G. (2010). Electrospun nanomaterials for ultrasensitive sensors. *Materials Today*, *13*, 16–27.

Girod Fullana, S., Ternet, H., Freche, M., Lacout, J. L., & Rodriguez, F. (2010). Controlled release properties and final macroporosity of a pectin microspheres–calcium phosphate composite bone cement. *Acta Biomaterialia*, *6*, 2294–2300.

Huang, W., Xu, H., Xue, Y., Huang, R., Deng, H., & Pan, S. (2012). Layer-by-layer immobilization of lysozyme-chitosan-organic rectorite composites on electrospun nanofibrous mats for pork preservation. *Food Research International*, *48*, 784–791.

Jayakumar, R., Prabaharan, M., Kumar, P., Nair, S., & Tamura, H. (2011). Biomaterials based on chitin and chitosan in wound dressing applications. *Biotechnology Advances*, *29*, 322–337.

Khang, D., Carpenter, J., Chun, Y. W., Pareta, R., & Webster, T. J. (2010). Nanotechnology for regenerative medicine. *Biomedical Microdevices*, *12*, 575–587.

Lin, H. Y., & Yeh, C. T. (2010). Controlled release of pentoxifylline from porous chitosan–pectin scaffolds. *Drug Delivery*, *17*, 313–321.

Ong, S. Y., Wu, J., Moochhala, S. M., Tan, M. H., & Lu, J. (2008). Development of a chitosan-based wound dressing with improved hemostatic and antimicrobial properties. *Biomaterials*, *29*, 4323–4332.

Pagán, J., Ibarz, A., Llorca, M., Pagán, A., & Barbosa-Cánovas, G. (2001). Extraction and characterization of pectin from stored peach pomace. *Food Research International*, *34*, 605–612.

Park, J. Y., Jung, Y. S., Cho, J., & Choi, W. K. (2006). Chemical reaction of sputtered Cu film with PI modified by low energy reactive atomic beam. *Applied Surface Science*, *252*, 5877–5891.

Rosso, M., Giesbers, M., Arafat, A., Schroën, K., & Zuilhof, H. (2009). Covalently attached organic monolayers on SiC and Si × N4 surfaces: Formation using UV light at room temperature. *Langmuir*, *25*, 2172–2180.

Rujitanaroj, P., Pimpha, N., & Supaphol, P. (2008). Wound-dressing materials with antibacterial activity from electrospun gelatin fiber mats containing silver nanoparticles. *Polymer*, *49*, 4723–4732.

Schiffman, J. D., & Schauer, C. L. (2008). A review: Electrospinning of biopolymer nanofibers and their applications. *Polymer Reviews*, *48*, 317–352.

Shalumon, K., Anulekha, K., Nair, S. V., Chennazhi, K., & Jayakumar, R. (2011). Sodium alginate/poly (vinyl alcohol)/nano ZnO composite nanofibers for antibacterial wound dressings. *International Journal of Biological Macromolecules*, *49*, 247–254.

Tripathi, S., Mehrotra, G., & Dutta, P. (2010). Preparation and physicochemical evaluation of chitosan/poly (vinyl alcohol)/pectin ternary film for food-packaging applications. *Carbohydrate Polymers*, *79*, 711–716.

Venugopal, J., & Ramakrishna, S. (2005). Biocompatible nanofiber matrices for the engineering of a dermal substitute for skin regeneration. *Tissue Engineering*, *11*, 847–854.

Wang, D., Liu, N., Xu, W., & Sun, G. (2011). Layer-by-layer structured nanofiber membranes with photoinduced self-cleaning functions. *The Journal of Physical Chemistry C*, *115*, 6825–6832.

Wang, X., Du, Y., Yang, J., Shi, X., & Hu, Y. (2006). Preparation, characterization and antimicrobial activity of chitosan/layered silicate nanocomposites. *Polymer*, *47*, 6738–6744.

Wang, X., Pei, X., Du, Y., & Li, Y. (2008). Quaternized chitosan/rectorite intercalative materials for a gene delivery system. *Nanotechnology*, *19*, 375102.

Xin, S., Li, Y., Li, W., Du, J., Huang, R., Du, Y., et al. (2012). Carboxymethyl chitin/organic rectorite composites based nanofibrous mats and their cell compatibility. *Carbohydrate Polymers*, *90*, 1069–1074.

Xu, R., Feng, X., Li, W., Xin, S., Wang, X., Deng, H., et al. (2013). Novel polymer-layered silicate intercalated composite beads for drug delivery. *Journal of Biomaterials Science. Polymer Edition*, *24*, 1–14.

Yang, T. C., Chou, C. C., & Li, C. F. (2002). Preparation, water solubility and rheological property of the N-alkylated mono or disaccharide chitosan derivatives. *Food Research International*, *35*, 707–713.

Zahedi, P., Rezaeian, I., Ranaei Siadat, S. O., Jafari, S. H., & Supaphol, P. (2010). A review on wound dressings with an emphasis on electrospun nanofibrous polymeric bandages. *Polymers for Advanced Technologies*, *21*, 77–95.

Zhang, X., Yang, D., & Nie, J. (2008). Chitosan/polyethylene glycol diacrylate films as potential wound dressing material. *International Journal of Biological Macromolecules*, *43*, 456–462.

Zhao, Q. S., Ji, Q. X., Xing, K., Li, X. Y., Liu, C. S., & Chen, X. G. (2009). Preparation and characteristics of novel porous hydrogel films based on chitosan and glycerophosphate. *Carbohydrate Polymers*, *76*, 410–416.

Zhou, S., Wang, L., & Xue, Q. (2011). Improvement in load support capability of aC (Al)-based nanocomposite coatings by multilayer architecture. *Surface and Coatings Technology*, *206*, 387–394.